Introduction to Neutron Stars

J. M. Lattimer

Department of Physics & Astronomy
Stony Brook University

2nd N3AS Neutron Stars Merger Meeting
September 23, 2021

Main Topics

- What is a neutron star?
- Neutron stars and their relation to the equation of state
- Maximum mass, causality and neutron matter constraints
- Neutron star masses and radii: radio, X-ray and gravitational wave observations
- Neutron star interior composition from observations: neutron star cooling

Dany Page
UNAM

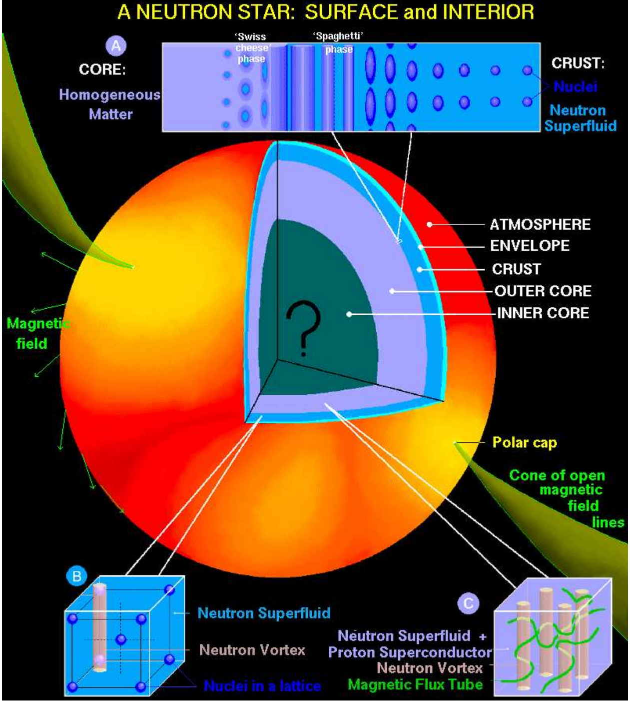

Neutron Stars: The History

1932 Landau suggests the existence of giant nucleus stars.
1932 Chadwick discovers the neutron.
1934 Baade & Zwicky predict the existence of neutron stars (NSs) as the end products of supernovae.
1939 Oppenheimer and Volkoff predict the upper mass limit of NS.
1964 Hoyle, Narlikar and Wheeler predict NSs rapidly rotate.
1964 Prediction that NSs have intense magnetic fields.
1966 Colgate and White incorporate neutrinos into supernova hydrodynamics.
1966 Wheeler predicts the Crab nebula is powered by a rotating NS.
1967 Pacini makes the first magnetic pulsar model.
1967 C. Schisler discovers a dozen pulsing radio sources, including one in the Crab pulsar, using secret military radar in Alaska.
1967 Hewish et al. discover first pulsar PSR 1919+21, Aug 6.
1968 Discovery of a pulsar in the Crab Nebula which was slowing down, ruling out binary models. Also clinched the connection with core-collapse supernovae.
1968 T. Gold identifies pulsars with rotating magnetized NSs.
1968 The term "pulsar" first appears in print, in the *Daily Telegraph*.
1969 Vela pulsar glitches observed; evidence for superfluidity in NSs.
1971 Accretion powered X-ray pulsar discovered by Uhuru (*not* the Lt.).
1974 Hewish awarded Nobel Prize (but Jocelyn Bell Burnell was not).
1974 Lattimer & Schramm suggest NS mergers make the r-process.

Neutron Stars: Later Discoveries

1974 First binary pulsar, PSR 1913+16, discovered by Hulse and Taylor.

1979 Taylor et al. observe orbital decay due to gravitational radiation in the PSR 1913+16 system, leading to their Nobel Prize in 1993.

1979 Chart recording of PSR 1919+21 used as album cover for *Unknown Pleasures* by Joy Division (#19/100 greatest British albums ever).

1982 First millisecond pulsar, PSR B1937+21, discovered by Backer et al.

1992 Wolszczan & Frail discover first exo-planets, orbiting PSR B1257+12.

1988 First black widow pulsar, PSR 1957+20, discovered by Fruchter et al.

1992 Duncan & Thompson predict existence of magnetars.

1996 Walter et al. discover closest known NS RXJ 1856-3754 at 61 pc.

2004 Magnetar SGR 1806-20: largest burst of energy in our Galaxy since Kepler's SN 1604, more than $L_\odot$ for 100,000 years.

2004 Hessels et al. discover the fastest (716 Hz) pulsar, PSR J1748-2446ad.

2005 Burgay et al. discover the first binary with two pulsars, PSR J0737-3039.

2013 Ransom et al. discover a pulsar in a triple system with 2 white dwarfs.

2017 Detection of first binary NS merger GW170817. Kilonova with probable r-process production observed.

2019 Cromartie et al.: most massive (2.07 $M_\odot$) NS, PSR J0740+6620.

2020 Discovery of first black hole-NS merger, GW200105 (but GW190426?).

Magnetic Dipole Model for Pulsars

A misaligned magnetic dipole ($\alpha > 0$) emits low-frequency electromagnetic radiation. Larmor formula for electric dipoles (charge q, acceleration $\dot{v}$) is

$$P_{rad} = \frac{2q^2\dot{v}^2}{3c^2} = \frac{2}{3c^3}(q\ddot{r}\sin\alpha)^2 = \frac{2\ddot{p}_\perp^2}{3c^2}$$

where $p_\perp$ is the perpendicular component of the electric dipole moment.

A uniformly magnetized sphere with radius R and surface field B has a magnetic dipole moment $|m| = BR^3$, and if rotating with period $P = 2\pi/\Omega$, has $m = |m|e^{-i\Omega t}$ and $|\ddot{m}| = \Omega^2|m|$. By analogy to an electric dipole,

$$P_{rad} = \frac{2}{3}\frac{\ddot{m}_\perp^2}{c^3} = \frac{2}{3c^2}\left(BR^3\sin\alpha\right)^2\left(\frac{2\pi}{P}\right)^4$$

This radiation appears at the low frequency $\nu = P^{-1} < 1$ kHz, too low to propagate throught the ionized ISM and be detected.

The total rotational energy and spin-down power, using $I = (2/5)MR^2$, are

$$E_{rot} = \frac{1}{2}I\Omega^2 \simeq 1.6\cdot 10^{50}\left(\frac{M}{M_\odot}\right)\left(\frac{R}{10\text{ km}}\right)^2\left(\frac{10\text{ ms}}{P}\right)^2\ \text{erg},$$

$$P_{rot} = -I\Omega\dot{\Omega} \simeq 1.6\cdot 10^{40}\left(\frac{M}{M_\odot}\right)\left(\frac{R}{10\text{ km}}\right)^2\left(\frac{10\text{ ms}}{P}\right)^3\left(\frac{-\dot{P}}{10^{-12}}\right)\ \text{erg s}^{-1}.$$

Magnetic Fields and Ages

Setting $P_{rad} = -P_{rot}$, one finds

$$B = \sqrt{\frac{3c^3 I P\dot{P}}{8\pi^2}\frac{1}{R^3}\frac{1}{\sin^2\alpha}} \simeq 2.9\cdot 10^{12}\left(\frac{10\ \mathrm{km}}{R\sin\alpha}\right)^2\sqrt{\frac{M}{M_\odot}\frac{P}{.01\ \mathrm{s}}\frac{\dot{P}}{10^{-12}}}\ \mathrm{G}$$

which is a minimum value since $\sin\alpha < 1$.

The **characteristic age** is estimated by assuming $P\dot{P} \simeq$ constant, or

$$\int_{P_0}^{P} PdP = P\dot{P}\int_0^\tau dt = P\dot{P}\tau = \frac{P^2 - P_0^2}{2},$$

giving, with $P_0 >> P$,

$$\tau = \frac{P}{2\dot{P}} \simeq 158\frac{P}{.01\ \mathrm{s}}\frac{10^{-12}}{\dot{P}}\ \mathrm{yr}.$$

A death line exists when the voltage $V \propto B\Omega^2$ near the polar cap drops below that needed to generate e^+e^- pairs:

$$\Phi = \frac{BR^3\Omega^2}{2c^2} \simeq 6.6\cdot 10^{16}\frac{B}{10^{12}\ \mathrm{G}}\left(\frac{0.01\ \mathrm{s}}{P}\right)^2\left(\frac{R}{10\ \mathrm{km}}\right)^3\ \mathrm{V}.$$

Note $BP^{-2} \propto \sqrt{\dot{P}P^{-3}} \propto P_{rot}$. Death line is where $BP^{-2} \sim 0.2\cdot 10^{12}$ G s^{-2}.

A $\log\dot{P} - \log P$ diagram for pulsars is like an H-R diagram for stars.

The $P - \dot{P}$ Diagram

$B \propto \sqrt{P\dot{P}}$
$\tau \propto P/\dot{P}$
$P_{rot} \propto P^{-3}\dot{P}$

The "death line" is
$P_{rot} \sim 10^{30}$ erg s^{-1}

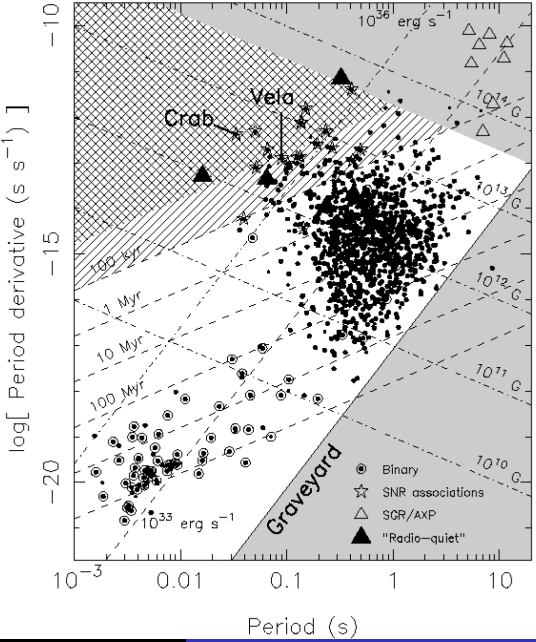

Taken from "Handbook of Pulsar Astronomy" by Lorimer & Kramer

Pulsar Flavors

Young PSRs

(high B, fast spin, very energetic)

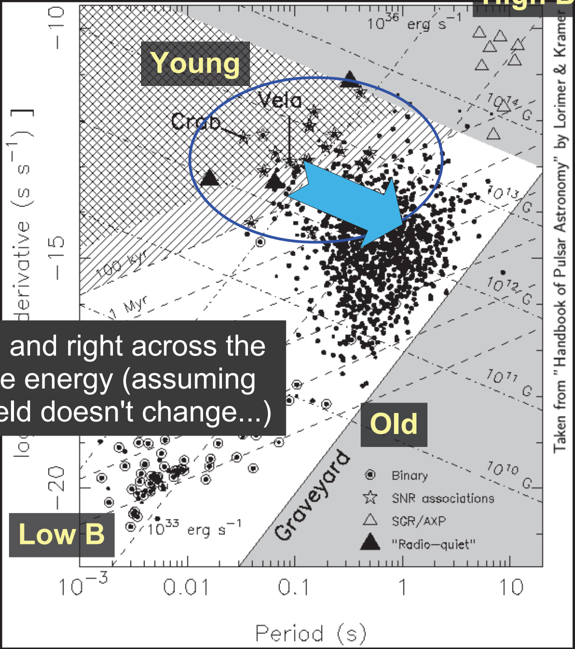

Pulsars move down and right across the diagram as they lose energy (assuming that the magnetic field doesn't change...)

Pulsar Flavors

Young PSRs

(high B, fast spin, very energetic)

Normal PSRs

(average B, slow spin)

Millisecond PSRs

(low B, very fast, very old, very stable spin, best for basic physics tests)

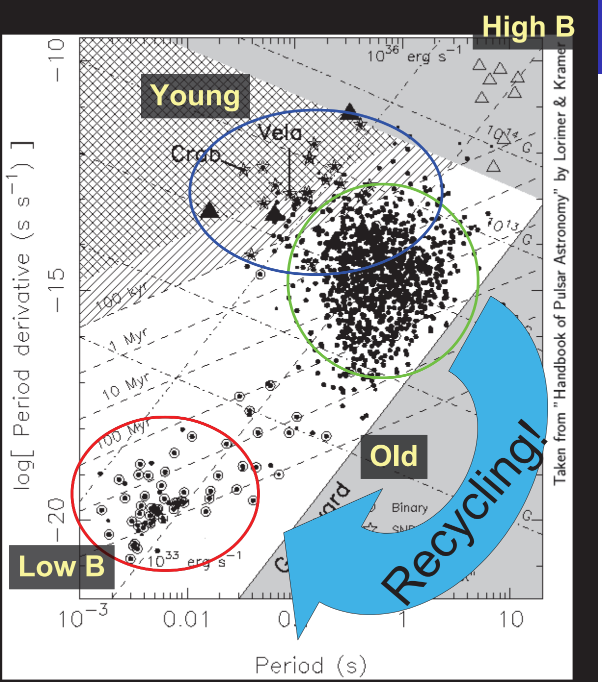

What's a Magnetar?

Neutron stars with extremely strong magnetic fields:

$10^{14\text{-}15}$ Gauss

(~1000x stronger than normal PSRs)

Powered by decay of magnetic field, not rotation!

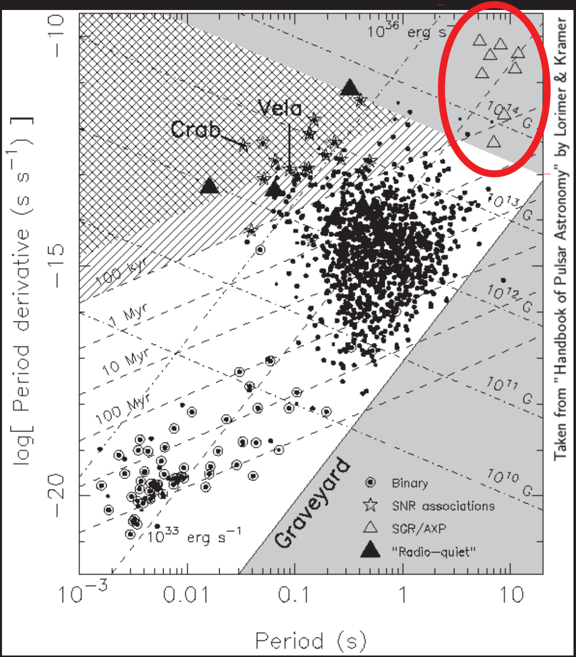

Giant X-ray Flares: Magnetar SGR 1900+14

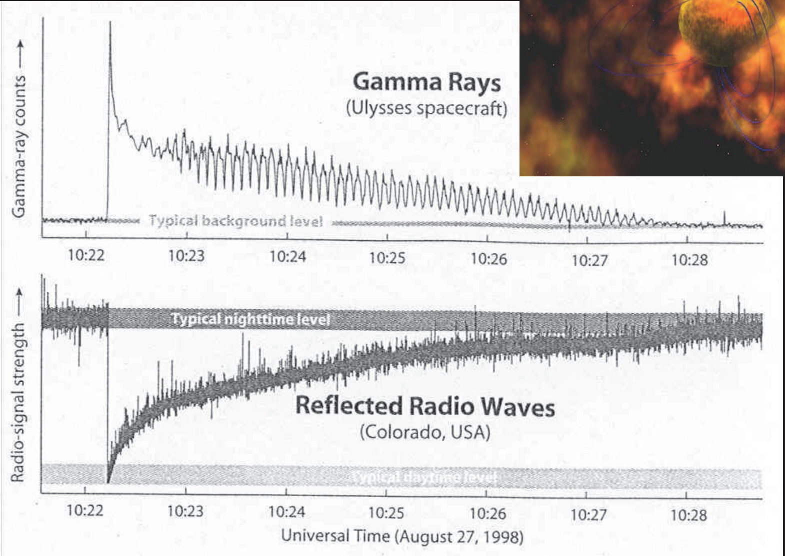

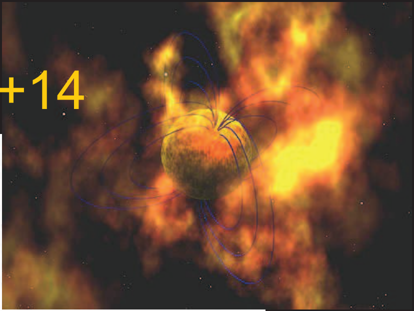

Pulsars are Precise Clocks

PSR J0437-4715

At 00:00 UT Jan 18 2011:

P = 5.7574519420243 ms
+/- 0.0000000000001ms

The last digit changes by 1 every half hour!

This digit changes by 1 every 500 years!

This extreme precision is what allows us to ***use pulsars as tools*** to do unique physics!

Pulsar Timing: *Pulse Phase Tracking*

Unambiguously account for every rotation of a pulsar over years

Measurement - Model = Timing Residuals

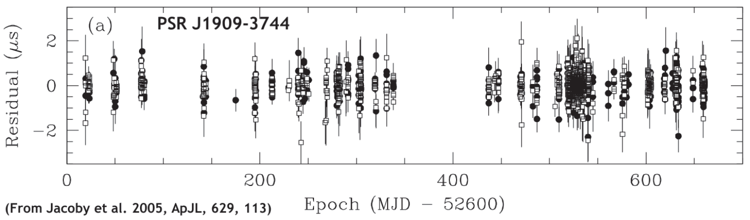

(From Jacoby et al. 2005, ApJL, 629, 113)

200ns RMS over 2 yrs

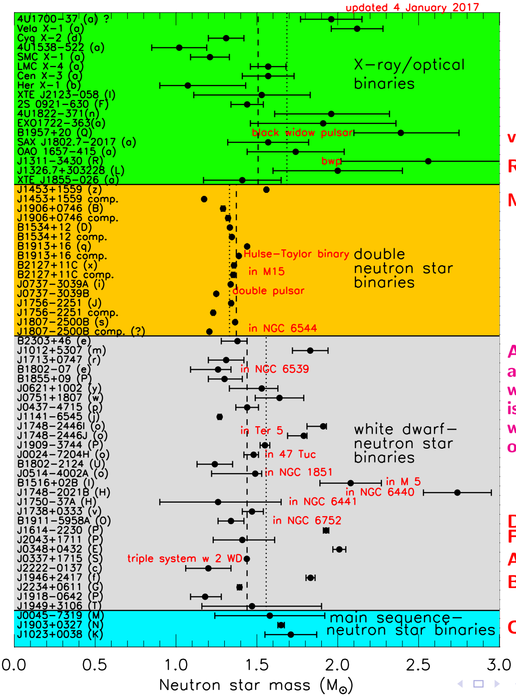

van Kerkwijk 2010

Romani et al. 2012

Martinez et al. 2015

Although simple average mass of w.d. companions is 0.23 $M_\odot$ larger, weighted average is only 0.07 $M_\odot$ larger.

Demorest et al. 2010
Fonseca et al. 2016

Antoniadis et al. 2013

Barr et al. 2016

Champion et al. 2008

Tolman-Oppenheimer-Volkov equations

$$\frac{dp}{dr} = -\frac{G}{c^4}\frac{(mc^2 + 4\pi pr^3)(\varepsilon + p)}{r(r - 2Gm/c^2)}$$

$$\frac{dm}{dr} = 4\pi\frac{\varepsilon}{c^2}r^2$$

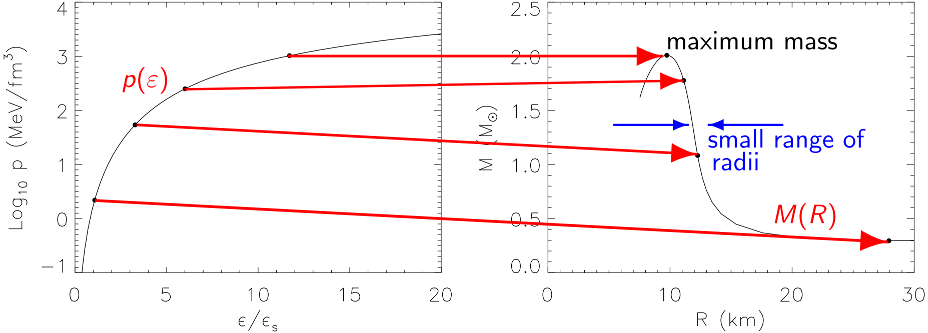

Equation of State ⟵ Observations

Mass-Radius Diagram and Theoretical Constraints

GR:

$R > 2GM/c^2$

$P < \infty$:

$R > (9/4)GM/c^2$

causality:

$R \gtrsim 2.9GM/c^2$

— normal NS

— SQS

— $R_\infty = \frac{R}{\sqrt{1-2GM/Rc^2}}$

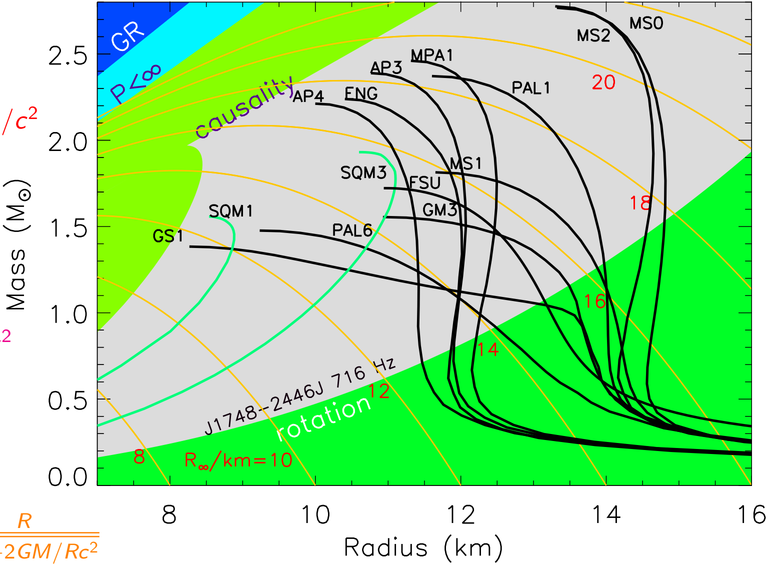

Extremal Properties of Neutron Stars

The most compact and massive configurations occur when the low-density equation of state is "soft" and the high-density equation of state is "stiff" (Koranda, Stergioulas & Friedman 1997).

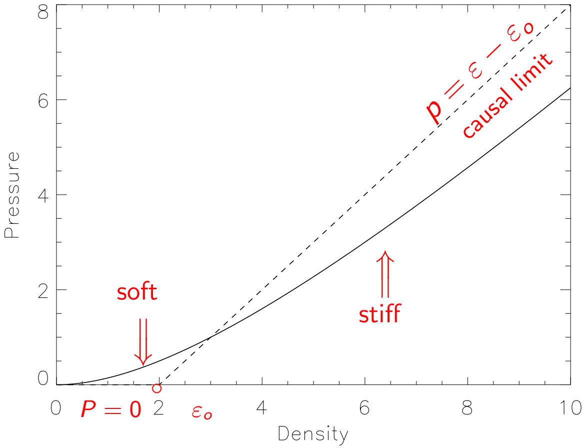

ε_o is the only EOS parameter

The TOV solutions scale with ε_o

Extremal Properties of Neutron Stars

A useful reference is the nuclear saturation density (interior density of normal nuclei): $\rho_s = 2.7 \times 10^{14}$ g cm^{-3}, $n_s = 0.16$ baryons fm^{-3}, $\varepsilon_s = 150$ MeV fm^{-3}

$$M_{\rm max} = 4.1\ (\varepsilon_s/\varepsilon_o)^{1/2} M_\odot \quad \text{(Rhoades \& Ruffini 1974)}$$

$$M_{B,\rm max} = 5.41\ (m_B c^2/\mu_o)(\varepsilon_s/\varepsilon_o)^{1/2} M_\odot$$

$$R_{\rm min} = 2.82\ GM/c^2 = 4.3\ (M/M_\odot)\ \rm km$$

$$\mu_{b,\rm max} = 2.09\ \text{GeV}$$

$$\varepsilon_{c,\rm max} = 3.034\ \varepsilon_o \simeq 51\ (M_\odot/M_{\rm largest})^2\ \varepsilon_s$$

$$P_{c,\rm max} = 2.034\ \varepsilon_0 \simeq 34\ (M_\odot/M_{\rm largest})^2\ \varepsilon_s$$

$$n_{B,\rm max} \simeq 38\ (M_\odot/M_{\rm largest})^2\ n_s$$

$$\text{BE}_{\rm max} = 0.34\ M$$

$$P_{\rm min} = 0.74\ (M_\odot/M_{\rm sph})^{1/2}(R_{\rm sph}/10\ \rm km)^{3/2}\ ms = 0.20\ (M_{\rm sph,max}/M_\odot)\ ms$$

The Radius – Pressure Correlation

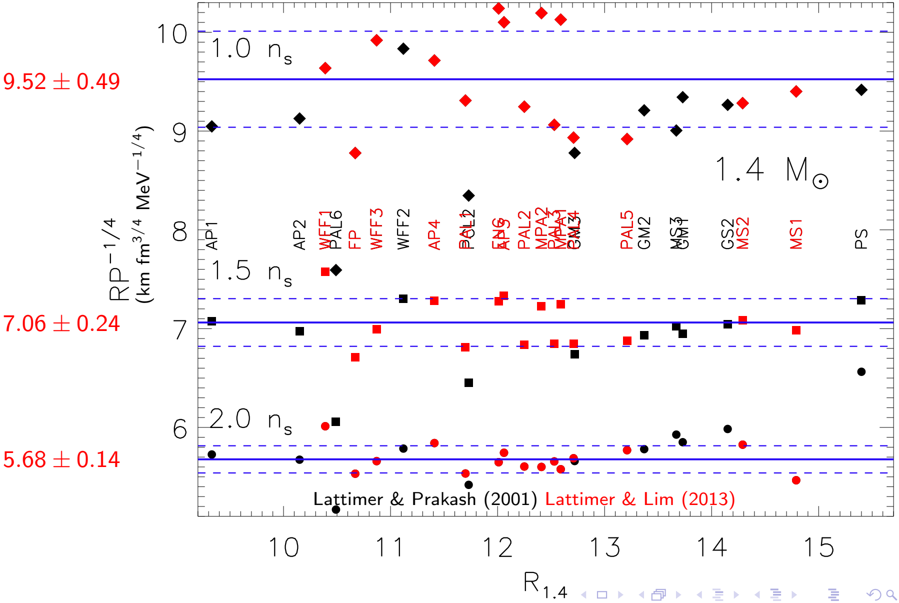

Nuclear Symmetry Energy and the Pressure

The symmetry energy is the difference between the energies of pure neutron matter ($x = 0$) and symmetric ($x = 1/2$) nuclear matter:

$$S(n) = E(n, x = 0) - E(n, x = 1/2)$$

Usually approximated as an expansion around the saturation density (n_s) and isopin symmetry ($x = 1/2$):

$$E(n, x) = E(n, 1/2) + (1 - 2x)^2 S_2(n) + \ldots$$

$$S_2(n) = \mathbf{S_v} + \frac{\mathbf{L}}{3}\frac{n - n_s}{n_s} + \ldots$$

$$\mathbf{S_v} \simeq 31 \text{ MeV}, \quad \mathbf{L} \simeq 50 \text{ MeV}$$

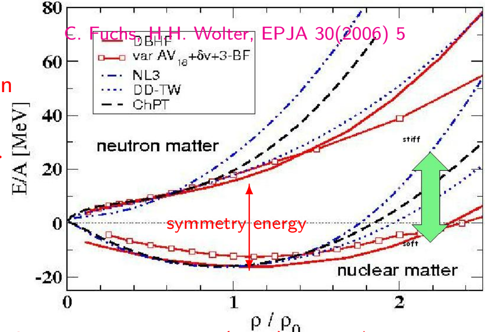

Extrapolated to pure neutron matter:

$$E_N = E(n_s, 0) \approx S_v + E(n_s, 1/2) \equiv S_v - B, \qquad P_N = P(n_s, 0) = L n_s/3$$

Neutron star matter (beta equilibrium) is nearly neutron matter:

$$\frac{\partial (E + E_e)}{\partial x} = 0, \quad P(n_s, x_\beta) \simeq \frac{L n_s}{3}\left[1 - \left(\frac{4 S_v}{\hbar c}\right)^3 \frac{4 - 3 S_v/L}{3\pi^2 n_s}\right]$$

Theoretical Neutron Matter Studies

Recently developed chiral effective field theory allows a systematic expansion of nuclear forces at low energies based on the symmetries of quantum chromodynamics. It exploits the gap between the pion mass (the pseudo-Goldstone boson of chiral symmetry-breaking) and the energy scale of short-range nuclear interactions established from experimental phase shifts. It provides the only known consistent framework for estimating energy uncertainties.

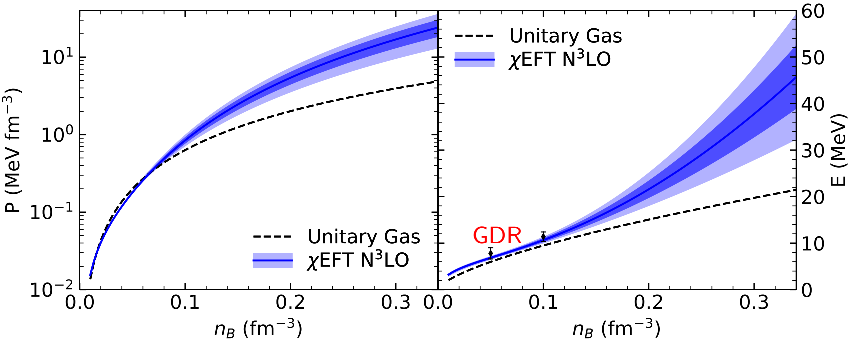

Bounds From The Unitary Gas Conjecture

The Conjecture:
Neutron matter energy is larger than that of the unitary gas $E_{UG} = \xi_0 (3/5) E_F$, or

$$E_{UG} \simeq 12.6 \left(\frac{n}{n_s}\right)^{2/3} \mathrm{MeV}$$

The unitary gas consists of fermions interacting via a pairwise short-range s-wave interaction with infinite scattering length and zero range. Cold atom experiments show a universal behavior with the Bertsch parameter $\xi_0 \simeq 0.37$.

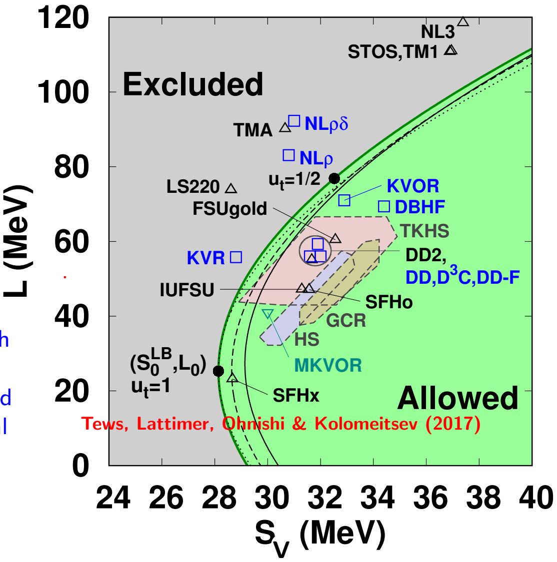

$S_v \geq 28.6$ MeV; $L \geq 25.3$ MeV; $P_N(n_s) \geq 1.35$ MeV fm^{-3}; $R_{1.4} \geq 9.7$ km

Nuclear Physics Constraints

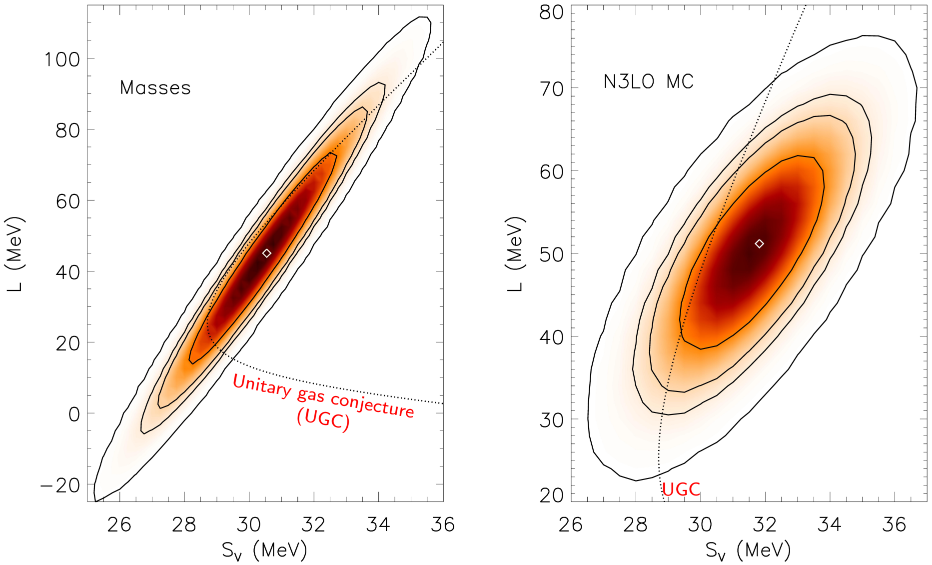

Combined Nuclear Physics Constraints

Predicted $L = 51 \pm 12$ MeV; $r_{np}^{208} = 0.17 \pm 0.04$ fm

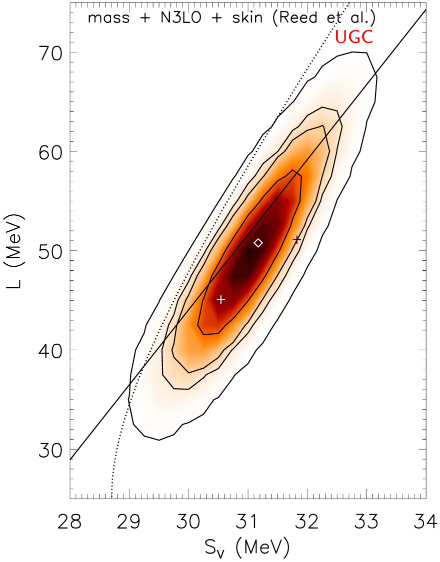

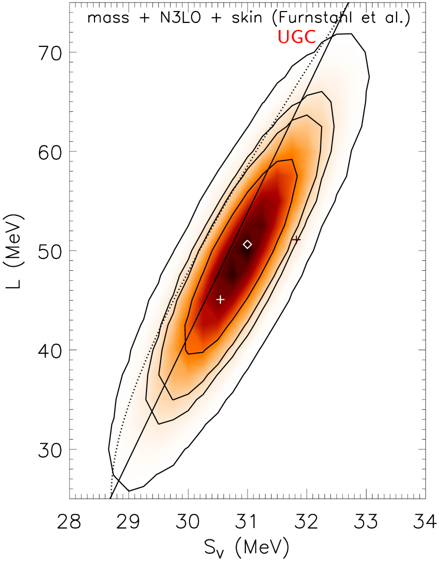

Measuring Neutron Star Masses and Radii

- Pulsar timing can accurately measure masses. Most are between $1.2M_\odot$ and $1.5M_\odot$; lowest well-measured mass is $1.174 \pm 0.004M_\odot$, highest are $2.07 \pm 0.07M_\odot$ and $2.01 \pm 0.04M_\odot$. Higher masses are found for some sources (notably black widow pulsars) but these estimates have large uncertainties.
- X-ray observations yield radii, but uncertain to a few km.
  - Quiescent binary sources in globular clusters
  - Thermonuclear explosions leading to photospheric radius expansion bursters on accreting neutron stars in binaries
  - Pulse profile modeling of hot spots on rapidly rotating neutron stars, e.g., Neutron Star Interior Composition ExploreR (NICER) mission.
- Gravitational waves from merging binary neutron stars (BNS) measure masses and tidal deformabilites.

Simultaneous Mass/Radius Measurements

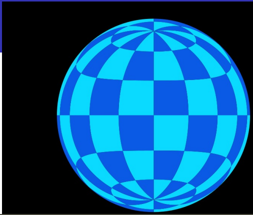

Measurements of flux $F_\infty = (R_\infty/D)^2 \sigma T_{\rm eff}^4$ and color temperature $T_c \propto \lambda_{\rm max}^{-1}$ yield an apparent angular size (pseudo-BB):

$$R_\infty/D = (R/D)/\sqrt{1 - 2GM/Rc^2}$$

Observational uncertainties include distance D, nonuniform T, interstellar absorption N_H, and atmospheric composition.

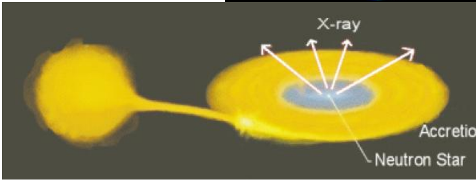

Best chances are:

Isolated neutron stars with parallax (atmosphere ??).
RX J1856-3754: $D = 115 \pm 8$ pc (Walter et al. 2010),
$R_\infty = 14.3 \pm 1.0$ km for H atmosphere (Ho et al. 2007).

Quiescent low-mass X-ray binaries (QLMXBs) in globular clusters (reliable distances, low B H-atmospheres).

Bursting sources with peak fluxes close to Eddington limit (PREs) where gravity balances radiation pressure.

Neutron Star Interior Composition ExploreR (NICER)

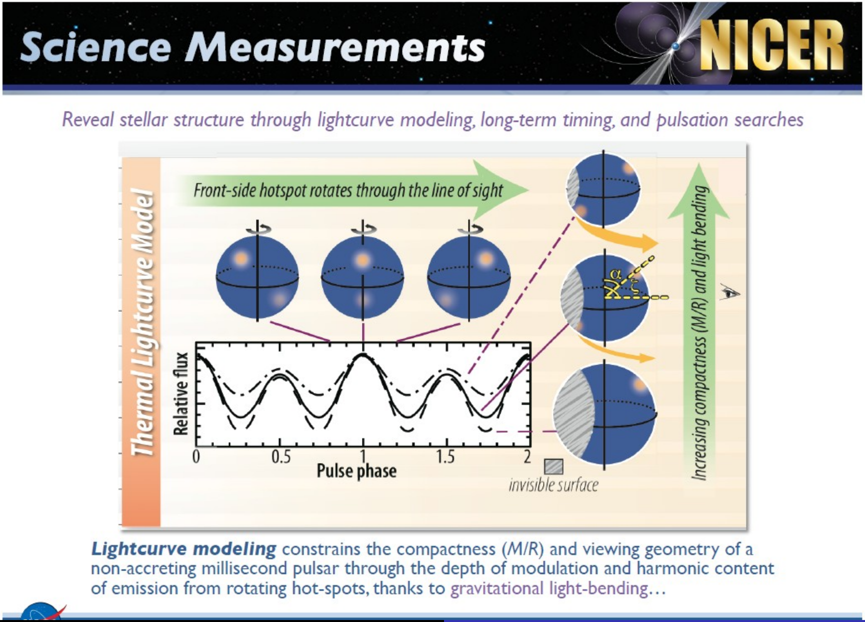

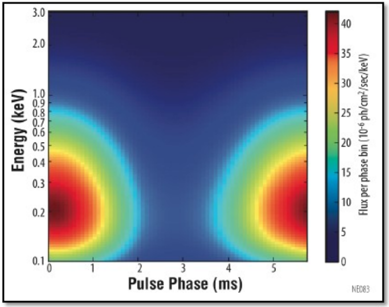

… while phase-resolved spectroscopy promises a direct constraint of radius *R*.

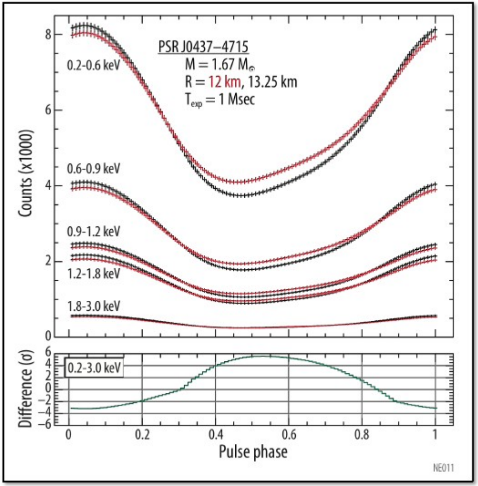

NICER: PSR J0030+0451

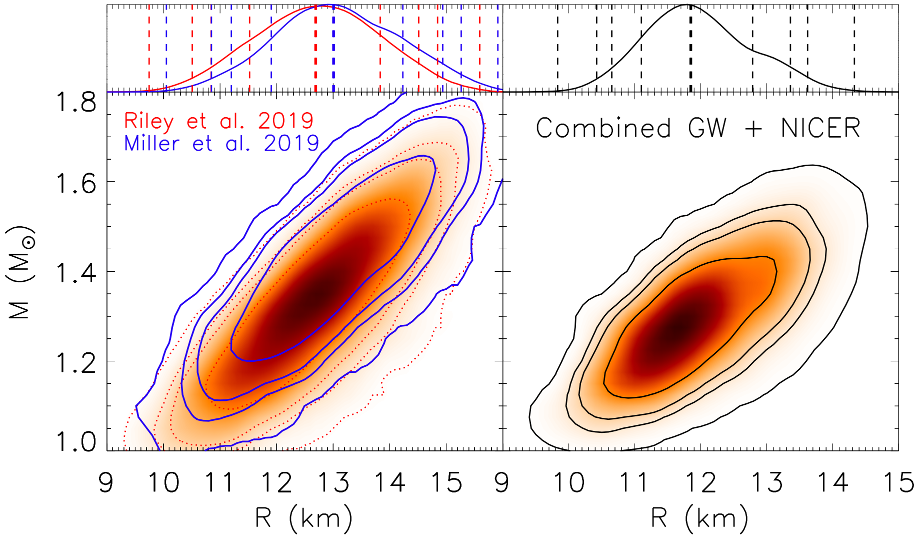

NICER: PSR J0740+6620

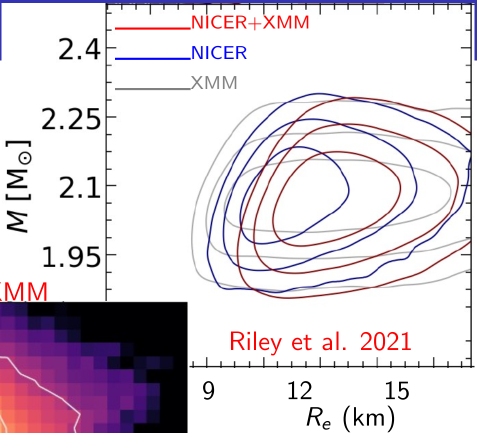

Riley et al. 2021

Miller et al. 2021

NICER

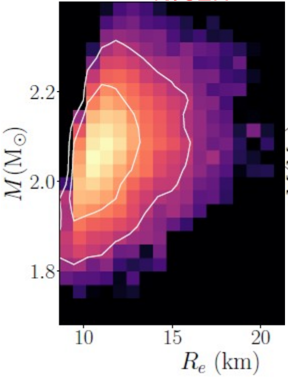

NICER+XMM

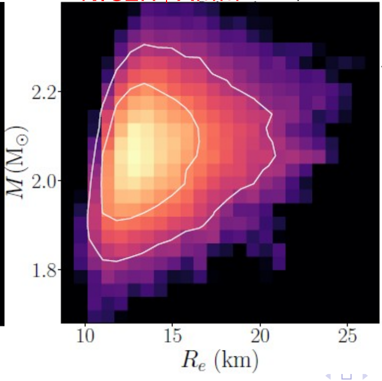

GW170817

Waveform analysis by De et al. (2018)

Zhao and Lattimer (2019)

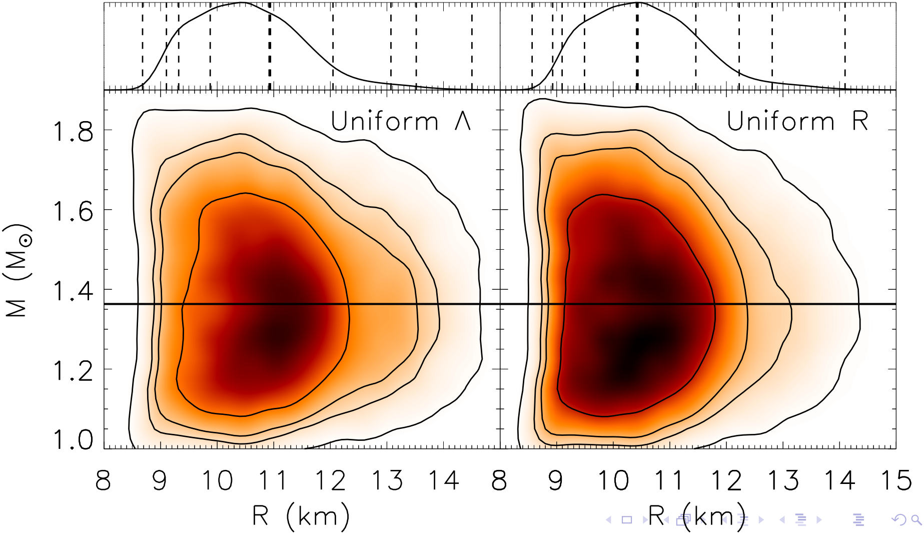

Neutron Star Cooling

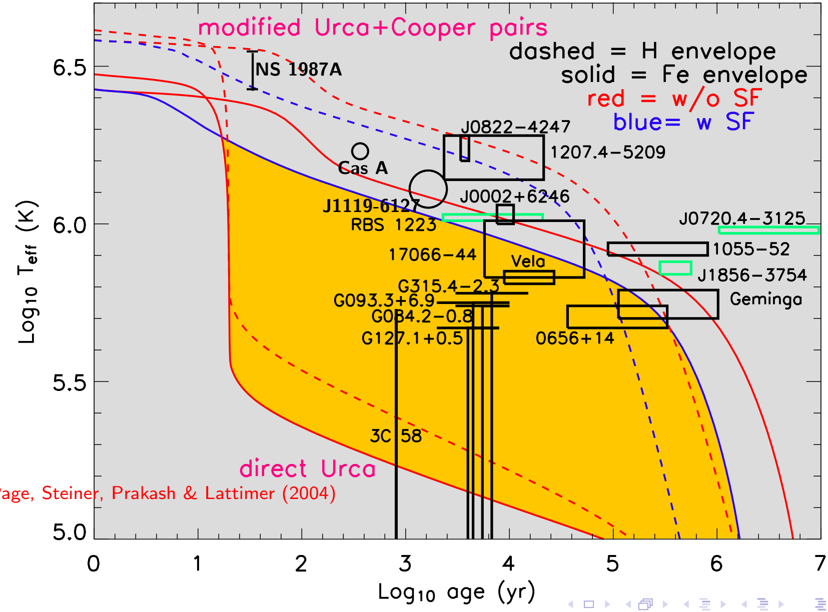

What We Learn From Cooling Observations

Most observed stars Atmospheric/envelope compositions are a mixture of light and heavy compositions. Most stars are consistent with n $^3P_2$ and p $^1S_0$ superfluidity in the core and n $^1S_0$ superfluidity in the crust, with relatively small superfluid gaps.

Cas A More-rapid-than-expected cooling implies that n $^3P_2$ superfluidity began a short time ago in the neutron star core, and that in the future (20-50 yrs) the cooling will slow to reflect the modified URCA rate. The n $^3P_2$ superfluid gap is of order $5 \cdot 10^8$ K; core p $^1S_0$ superfluidity began a long time ago and has a higher-temperature gap. Direct URCA cooling is not taking place. Atmospheric composition is probably light-element (C).

NS 1987A Revealed through the extra heating of a dust blob in which it is embedded. It is unlikely direct URCA cooling is taking place. The atmosphere composition is consistent with light elements. Both NS 1987A and Cas A could be on very similar cooling trajectories. Other observations indicate they have similar masses, near $1.4 - 1.6 M_\odot$.